Eur. Phys. J. A **10**, 267–273 (2001)

THE EUROPEAN PHYSICAL JOURNAL A

Generalized hybrid derivative coupling model for finite nuclei

B. Malakar[1] and G. Gangopadhyay[2,a]

[1] Department of Theoretical Physics, Indian Association for Cultivation of Science, Jadavpur, Calcutta 700 032, India
[2] Department of Physics, University College of Science, University of Calcutta, 92 Acharya Prafulla Chandra Road, Calcutta 700 009, India

Received: 18 August 2000 / Revised version: 18 February 2001
Communicated by P. Schuck

Abstract. The generalized hybrid derivative coupling model has been applied to explore various ground state properties of different nuclei. In this work we have confined our calculation only to the model characterized by the hybridization parameter $\alpha = 1/4$ which gives better results than the other models of the same class, as we have seen earlier, for nuclear matter calculations. The binding energy, single-particle energy spectra, density and charge radii of different doubly closed nuclei like ^{16}O, ^{40}Ca, ^{48}Ca, ^{90}Zr, ^{132}Sn, ^{208}Pb have been studied. The success of this model, in describing the doubly closed nuclei, motivates us to extend this calculation further in the case of open shell nuclei after incorporating the pairing interaction and using a BCS transformation. We have calculated the binding energy for such nuclei. We have also studied the isotopic shift for different Pb isotopes with respect to ^{208}Pb. We have compared our results with the other standard theoretical results as well as with the experimental values.

PACS. 21.60.Jz Hartree-Fock and random-phase approximation – 21.10.Dr Binding energies and masses

1 Introduction

The purpose of this work is to study the ground state properties of finite nuclei in the framework of the generalized hybrid derivative coupling model [1]. This model has already been applied to study the properties of symmetric and asymmetric nuclear matter at zero and finite temperatures and also the phase transition from nuclear matter to quark matter and from neutron matter to quark matter [2, 3]. In the generalized hybrid derivative coupling model [1] both Yukawa point coupling and derivative coupling between the baryon wave function and the scalar meson are used in the Lagrangian but with unequal strengths unlike the hybrid derivative coupling model proposed by Glendenning *et al.* [4], where the scalar meson couples with equal strength to the baryon wave function and its derivative. The idea of derivative coupling, in nuclear matter problem, was first introduced by Zimanyi and Moszkowski [5] to remedy the defects (high bulk modulus and low nucleon effective mass) of the linear σ-ω model originally proposed by Walecka [6], where only Yukawa point coupling between the nucleon and the baryon wave function is assumed. But this model (hereafter referred to as ZM), when applied to finite nucleus, cannot reproduce the correct spin-orbit splitting. However, some variations of ZM model give better results in the case of finite nuclei [7]. Recently Hua *et al.* [8] obtained a better result for spin-orbit potential by introducing a tensor coupling term in the original Zimanyi-Moszkowski model [5]. However, they [8] have confined their calculations only to the case of spherical nucleus ^{208}Pb. In our model [1] we have taken the strength of the Yukawa point coupling and that of the derivative coupling in the ratio $(1-\alpha)/\alpha$, where α is called hybridization parameter.

Suitable values of the hybridization parameter α are chosen so that satisfactory results for nuclear matter properties like the compression modulus (K), effective nucleon mass M^*, binding energy per nucleon ($\epsilon/\rho - M$), symmetry energy $E_{\rm sym}$ and saturation nuclear matter density ρ_0 are reproduced. In our calculation we have found that the model characterized by $\alpha = 1/4$ can give better results than other models existing in the literature for infinite nuclear matter [1]. This has led us to apply it to study the properties of finite nuclei. In this work we shall focus our attention only on the model characterized by $\alpha = 1/4$ and compare our results with those obtained by different models and also with the experimental results.

We study the various ground state properties like the binding energy, single-particle energy spectra, density and charge radii of a number of magic nuclei. The present calculation gives a better result than any model which uses the same number of adjustable parameters. The generalized Wallecka model which includes the ρ meson and the photon, failed to reproduce the compressibility of nuclear

[a] e-mail: gautam@cucc.ernet.in

matter and the binding energy of finite nuclei [9,10]. Two nonlinear meson self-interaction terms had to be included for a correct description of the binding energy and the deformation of finite nuclei [9]. Thus, this model [9] requires eight parameters in contrast to seven parameters used in the hybrid derivative coupling model (including the hybridization parameter). A fit of the finite nuclear properties yet required a negative quartic term which makes the model unbounded from below [11]. In contrast, the derivative coupling model does not suffer from this problem. We also extend our calculation to open shell nuclei by including pairing and study a number of spherical nuclei throughout the periodic table. We would like to emphasize that the aim of the present work is to study the suitability of the generalized hybrid derivative coupling model to describe the properties of finite nuclei. So, no attempt has been made to modify the parameters by fitting the experimental data available on finite nuclei.

The paper is arranged as follows. In Section 2, we outline the theory and write down the necessary equations. The results of our calculations are presented next in Section 3. Finally, we summarize our findings and conclude in Section 4.

2 Theory

The details of the general form of the hybrid derivative coupling model have already been given in our earlier publications [1–3]. We give here a brief description of the above model for finite nucleus, where an additional contribution due to photon and its coupling to the proton is to be considered. We consider the following form of Lagrangian density for the finite nucleus:

$$\begin{aligned} L_{\rm initial} = \left(1+\alpha\frac{\sigma g_\sigma}{M}\right)\bar\psi\Bigg(& i\gamma_\mu\partial^\mu - g_\omega\omega^\mu\gamma_\mu \\ & -\frac{1}{2}g_\rho\gamma^\mu\vec\tau.\rho_\mu - e\frac{1+\tau_3}{2}A^\mu\gamma_\mu\Bigg)\psi \\ & -\Big[1-(1-\alpha)\frac{\sigma g_\sigma}{M}\Big]M\bar\psi\psi + \frac{1}{2}(\partial_\mu\sigma\partial^\mu\sigma - m_\sigma^2\sigma^2) \\ & -\frac{1}{4}\omega_{\mu\nu}\omega^{\mu\nu} + \frac{1}{2}m_\omega^2\omega_\mu\omega^\mu \\ & -\frac{1}{4}\rho_{\mu\nu}\rho^{\mu\nu} + \frac{1}{2}m_\rho^2\rho_\mu\rho^\mu - \frac{1}{4}A_{\mu\nu}A^{\mu\nu}\,, \end{aligned} \tag{1}$$

where ψ denotes a baryon (neutron and proton) wave function of mass M. σ, ω^μ, and ρ^μ are isoscalar scalar, isoscalar vector and isovector vector meson fields with masses m_σ, m_ω and m_ρ, respectively. The coupling constants for the σ-, the ω-, the ρ-mesons and for the photon (A^μ) are g_σ, g_ω, g_ρ and $e^2/4\pi = 1/137$, respectively. As usual the quantities $\omega^{\mu\nu}$, $\rho^{\mu\nu}$ and $A^{\mu\nu}$ are the antisymmetric field tensors for the ω-, ρ-mesons and for the electromagnetic field, respectively. Equation (1) implies that the ratio of the strength of Yukawa point coupling and that of the derivative coupling is given by $(1-\alpha)/\alpha$. A suitable value of α may be chosen to give satisfactory results for the bulk properties of nuclear matter. It is also evident from eq. (1) that there is coupling between the scalar meson and the vector meson. The above Lagrangian is Lorentz invariant but not renormalizable. However, as the nuclear field theory is an effective theory, this nonrenomalizibility of the Lagrangian may not be a "weighty objection" [4]. However, we will not use the above Lagrangian $L_{\rm initial}$ in this paper, rather we will work with the following transformed Lagrangian:

$$\begin{aligned} L = \bar\psi\Big(& i\gamma_\mu\partial^\mu - M^* - g_\omega\omega^\mu\gamma_\mu \\ & -\frac{1}{2}g_\rho\gamma^\mu\vec\tau.\rho_\mu - e\frac{1+\tau_3}{2}A^\mu\gamma_\mu\Big)\psi \\ & +\frac{1}{2}(\partial_\mu\sigma\partial^\mu\sigma - m_\sigma^2\sigma^2) - \frac{1}{4}\omega_{\mu\nu}\omega^{\mu\nu} + \frac{1}{2}m_\omega^2\omega_\mu\omega^\mu \\ & -\frac{1}{4}\rho_{\mu\nu}\rho^{\mu\nu} + \frac{1}{2}m_\rho^2\rho_\mu\rho^\mu - \frac{1}{4}A_{\mu\nu}A^{\mu\nu}\,, \end{aligned} \tag{2}$$

which has been obtained from (1) by rescaling [1,4,5] the baryon wave function in the following way:

$$\psi \rightarrow \left(1+\alpha\frac{\sigma g_\sigma}{M}\right)^{-1/2}\ \psi\,. \tag{3}$$

The effective nucleon mass occurring in (2) is given by

$$M^* = \frac{1-(1-\alpha)\sigma g_\sigma/M}{1+\alpha\sigma g_\sigma/M}M\,. \tag{4}$$

Here, we shall treat the Lagrangian (2) in the frequently used mean-field approximation (Hartree) in which the meson fields σ, ω_μ, ρ_μ and A_μ behave as classical fields and the nucleons as point-like particles. Using time reversal symmetry it is possible to eliminate the spatial vector components of ω_μ, ρ_μ and A_μ and only the time-like components ω_0, ρ_0 and A_0 will contribute. Furthermore, for static solutions the meson fields are time independent. Under these approximations and by the classical variational principle, the equations of motion for the meson as well as nucleons are

$$(-\bigtriangledown^2+m_\sigma^2)\sigma(\mathbf{r}) = g_\sigma\left(1+\alpha\frac{\sigma g_\sigma}{M}\right)^{-2}\rho_s(\mathbf{r}) = g_\sigma\rho_s'(\mathbf{r})\,, \tag{5}$$

$$(-\bigtriangledown^2+m_\omega^2)\omega_0(\mathbf{r}) = g_\omega\rho_B(\mathbf{r})\,, \tag{6}$$

$$(-\bigtriangledown^2+m_\rho^2)\rho_0(\mathbf{r}) = \frac{1}{2}g_\rho\rho_3(\mathbf{r})\,, \tag{7}$$

$$-\bigtriangledown^2 A_0(\mathbf{r}) = e\rho_p(\mathbf{r})\,, \tag{8}$$

and

$$\Big\{i\gamma^\mu\partial_\mu - M^* - \gamma_0\Big[e\frac{(1+\tau_3)}{2}A^0 + g_\omega\omega_0 + \frac{1}{2}g_\rho\tau_3\rho_0\Big]\Big\}\psi_\beta = 0\,. \tag{9}$$

Among the Klein-Gordon equations, only the first equation is different from the conventional RMF equations while the Dirac equation differs in the expression of the effective mass term. In the present work, we restrict

ourselves to the case of spherically symmetric mean fields *i.e.* $\sigma(\mathbf{r}) = \sigma(r)$, etc. The different densities occurring in the above eqs. (5)-(8), after the inclusion of the pairing interaction through BCS technique, have the standard form as in other RMF calculations. We have used the constant gap approach with the gap being taken following the prescription [12] $\Delta = 11.2/\sqrt{Z(N)}$ for proton (neutron) for open shell.

The nuclear radial wave functions are then determined by the following coupled differential equations:

$$\frac{\mathrm{d}}{\mathrm{d}r}G_\beta(r) + \frac{\kappa}{r}G_\beta(r) - \Big[\epsilon_\beta - g_\omega\omega_0(r) - \frac{1}{2}g_\rho\rho_0(r)\tau_{0\beta} - eA_0(r)\frac{1+\tau_{0\beta}}{2} + \{M - (1-\alpha)g_\sigma\sigma(r)\}\Big(1+\alpha\frac{g_\sigma}{M}\sigma(r)\Big)^{-1}\Big] \times F_\beta(r) = 0\,, \tag{10}$$

$$\frac{\mathrm{d}}{\mathrm{d}r}F_\beta(r) - \frac{\kappa}{r}F_\beta(r) + \Big[\epsilon_\beta - g_\omega\omega_0(r) - \frac{1}{2}g_\rho\rho_0(r)\tau_{0\beta} - eA_0(r)\frac{1+\tau_{0\beta}}{2} - \{M - (1-\alpha)g_\sigma\sigma(r)\}\Big(1+\alpha\frac{g_\sigma}{M}\sigma(r)\Big)^{-1}\Big] \times G_\beta(r) = 0\,, \tag{11}$$

where G_β and F_β are the radial wave functions for the upper and lower components of the Dirac spinor ψ_β given by

$$\psi_\beta(\mathbf{r}) = \begin{pmatrix} iG_\beta(r)\Phi_\beta(\theta,\phi,s)/r \\ -F_\beta(r)\Phi_{-\beta}(\theta,\phi,s)/r \end{pmatrix}\eta_t\,, \tag{12}$$

where the symbols have the usual meaning. They are normalized to

$$\int_0^\infty \mathrm{d}r\{\mid G_\beta\mid^2 + \mid F_\beta\mid^2\} = 1\,. \tag{13}$$

Instead of the term $g_\sigma\sigma$ as in the Walecka model [6] or $g_\sigma\sigma/(1+g_\sigma\sigma/M)$ as in the Zimanyi-Moszkowski model [5] or $g_\sigma\sigma/2(1+g_\sigma\sigma/2M)^{-1}$ as in the Glendenning model [4], the nucleon equations in (10)-(11) have the term $\sigma g_\sigma(1-\alpha)(1+\alpha\frac{g_\sigma}{M}\sigma)^{-1}$ in the generalized hybrid derivative coupling model. Actually the essential difference lies in the σ field equation (5) which has now become nonlinear.

The problem is treated in the coordinates space. The above coupled nonlinear differential equations (5)-(8) and (10)-(11) for finite spherical nuclei are solved by an iterative method. For a given set of potentials for the mesons, Dirac equations (10) and (11) may be solved to determine the eigenvalues ϵ_β. Once the nuclear wave functions have been calculated and inserted, the source terms may be calculated in the usual manner. Equations (5)-(8) then may be solved and improved values of the fields obtained, which are again inserted in the Dirac equations (10) and (11). This continues until the solution converges. The iteration is started with a Woods-Saxon potential for the meson fields.

The total binding energy is given by

$$E = E_{\mathrm{nucl}} + E_\sigma + E_\omega + E_\rho + E_{\mathrm{Coul}} - E_{\mathrm{c.m.}} + E_{\mathrm{pair}} - AM \tag{14}$$

with

$$E_{\mathrm{nucl}} = \sum_\beta \epsilon_\beta w_\beta\,, \tag{15}$$

$$E_\sigma = \frac{1}{2}\int \mathrm{d}^3r\sigma g_\sigma\rho_s'\,, \tag{16}$$

$$E_\omega = -\frac{1}{2}\int \mathrm{d}^3r\omega_0 g_\omega\rho_B\,, \tag{17}$$

$$E_\rho = -\frac{1}{4}\int \mathrm{d}^3r\rho_0 g_\rho\rho_3\,, \tag{18}$$

$$E_{\mathrm{Coul}} = -\frac{1}{2}\int \mathrm{d}^3rA_0 e\rho_p\,, \tag{19}$$

$$E_{\mathrm{c.m.}} = \frac{3}{4}41\ A^{-1/3}\ \mathrm{MeV}\,, \tag{20}$$

$$E_{\mathrm{pair}} = -\Delta\sum_\beta\sqrt{w_\beta(1-w_\beta)}\,. \tag{21}$$

Here $E_{\mathrm{c.m.}}$ is nothing but the zero-point energy correction term that arises due to the nonrelativistic centre-of-mass motion in the mean field and A is the nucleon number. E_{pair} is the pairing energy.

The charge radius (in fm) can be calculated by using the following simple relation:

$$r_c = \sqrt{r_p^2 + 0.65}\,. \tag{22}$$

The factor 0.65 in eq. (22) accounts for the finite-size effects of the proton. Taking into account the finite size of the proton, the charge density ρ_p is calculated by the folding integral:

$$\rho_{\mathrm{ch}}(\mathbf{r}) = \int \rho_p(\mathbf{r}')g(\mathbf{r}-\mathbf{r}')\mathrm{d}^3r'\,, \tag{23}$$

where the form factor $g(\mathbf{r})$ is given by

$$g(\mathbf{r}) = \frac{\mu^3}{8\pi}\exp[-\mu|\mathbf{r}|]\,, \tag{24}$$

with μ=845 MeV.

3 Results

The first task before us is to fix the parameters of the Lagrangian density of (2). There are six free parameters to be determined in the present approach, namely, the masses of the three mesons and the three coupling constants. In a

Table 1. The values of the different parameters assumed in the present calculation for the model characterized by $\alpha = 1/4$. The saturated nuclear matter properties for this parameter set are also included.

Meson masses			Coupling strengths			Saturated nuclear matter properties				
m_σ MeV	m_ω MeV	m_ρ MeV	g_σ^2	g_ω^2	g_ρ^2	ρ_0 fm^{-3}	$(\epsilon/\rho - M)$ MeV	$E_{\rm sym}$ MeV	M^* MeV	K MeV
526.0	783.0	763.0	73.741	94.565	69.932	0.159	-16	34	685.5	307

nuclear matter calculation there are three free parameters, given by

$$C_a^2 = \frac{g_a^2 M^2}{m_a^2}, \tag{25}$$

where the index a refers to σ, ω or ρ. The values of these parameters for the hybrid derivative coupling which reproduce the properties of the saturated nuclear matter have already been obtained [3]. Keeping those values unchanged means that only three parameters can be varied freely to reproduce the results for the finite nuclei. As our intention is to explore the applicability of the present Lagrangian density to describe the ground state properties of finite nuclei, we have not varied the meson masses to assume a good fit but, instead, assumed the usual values. Table 1 lists the values of the coupling constants and the meson masses and also the corresponding saturation nuclear matter properties for the model characterized by the hybridization parameter α=1/4. The nucleon mass is taken to be 939 MeV. The grid size is taken to be 0.04 fm.

We have used the present Lagrangian to calculate the different ground state properties of a number of doubly and singly closed shell nuclei throughout the periodic table. In table 2, we summarise the results obtained using the present approach as well as some other methods for a number of doubly closed shell nuclei. Here ZM refers to the original Zimanyi-Moszkowski model, ZM3 refers to the modified Zimanyi-Moszkowski model as applied in [7], GL refers to the hybrid derivative coupling model of Glendening *et al.* [4] and NL1 refers to the mean-field Lagrangian of [10] using the parameter set NL1. The next column (indicated by Pres.) shows the results obtained in the present calculation. For comparison, the experimental values are given in the last column. The first two results are taken from [7] after adding a correction due to the centre-of-mass energy. This correction makes the ZM3 calculation explain the binding energies better. The parameter sets for the first two results are given in [7]. The parameter set for GL has been fixed by using the parameters for the infinite nuclear matter from [4] and keeping the meson masses identical with the calculations cited earlier [7]. One can see that the present work gives a better description of the different experimental quantities than the first three calculations. Binding energies of almost all the nuclei are predicted more accurately than the first three methods. A better description of the spin-orbit splitting is obtained in almost all cases in our model. In short, the present model with $\alpha = 1/4$ gives the most accurate description of the different ground state properties of magic nuclei among other models which use the same number of parameters.

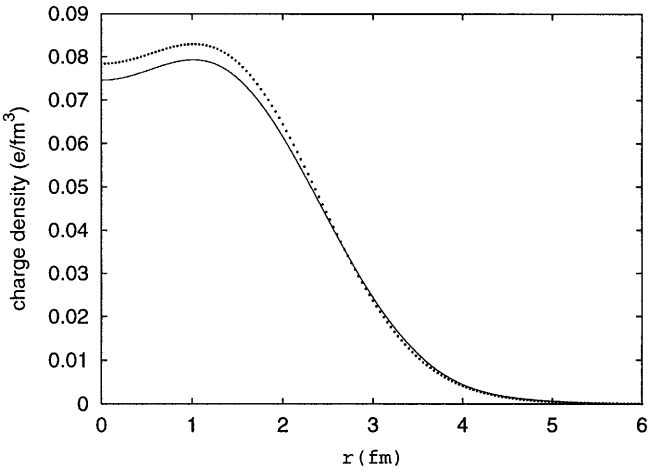

Fig. 1. Comparison of experimental and theoretically calculated charge density for ^{16}O as a function of radius. The solid line represents the experimental result taken from [13]. The dots represent theoretically calculated values.

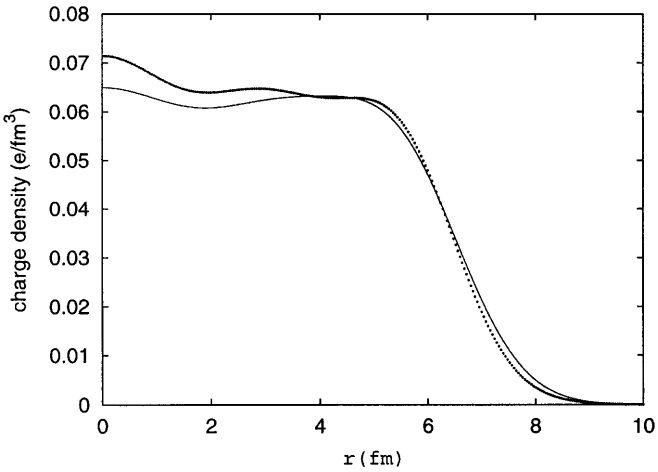

Fig. 2. Comparison of experimental and theoretically calculated charge density for ^{208}Pb as a function of radius. The solid line represents the experimental result taken from [13]. The dots represent theoretically calculated values.

In figs. 1 and 2, we plot the charge densities for ^{16}O and ^{208}Pb, respectively, calculated following the procedure discussed in the previous section and compare with the experimental charge distributions [13] (solid curve). Our calculation, in agreement with other relativistic works, shows a slight depression at the centre of the nucleus, a fact that has been verified by experiments. There is some uncer-

Table 2. Table showing different quantities for a number of closed shell nuclei calculated using different methods as well as the experimental values. All the energy values are in MeV and the radii are in fm. See text for more details.

Nucleus	Quantity	ZM[a]	ZM3[a]	GL	NL1[b]	Pres.	Expt.
^{16}O	B.E.	9.16	8.26	8.46	7.95	8.09	7.98
	$r_{\rm ch}$	2.64	2.78	2.63	2.77	2.65	2.73[c]
	$\Delta E(1p_{3/2}\text{-}1p_{1/2})$	1.4	2.8	2.2	6.1	3.3	6.1
^{40}Ca	B.E.	9.23	8.65	8.76	8.56	8.56	8.55
	$r_{\rm ch}$	3.39	3.51	3.35	3.50	3.38	3.48[c]
	$\Delta E(1d_{5/2}\text{-}1d_{3/2})$	1.5	3.1	2.3	6.8	3.5	6.3
^{48}Ca	B.E.	8.96	8.48	8.58	8.60	8.59	8.67
	$r_{\rm ch}$	3.47	3.57	3.41	3.49	3.43	3.47[c]
	$\Delta E(1d_{5/2}\text{-}1d_{3/2})$	1.1	2.5	1.9	6.4	3.0	3.6
^{90}Zr	B.E.	8.88	8.53	8.59	8.72	8.62	8.71
	$r_{\rm ch}$	4.25	4.35	4.17	4.28	4.24	4.27[c]
^{132}Sn	B.E.			8.27	8.32	8.26	8.35
	$r_{\rm ch}$			4.65	4.73	4.65	
^{208}Pb	B.E.	7.88	7.68	7.71	7.89	7.77	7.87
	$r_{\rm ch}$	5.54	5.66	5.41	5.52	5.42	5.50[c]
	$\Delta E(2p_{3/2}\text{-}2p_{1/2})$	0.4	0.9	0.4	1.1	0.6	0.5
	$\Delta E(2f_{7/2}\text{-}2f_{5/2})$	0.5	1.2	0.8	1.9	1.3	1.8
	$\Delta E(3p_{3/2}\text{-}3p_{1/2})$	0.2	0.4	0.3	0.8	0.4	0.9

[a] Taken from [7] after adding centre-of-mass energy correction.
[b] Using the parameter set NL1 [10].
[c] Taken from the compilation [13].

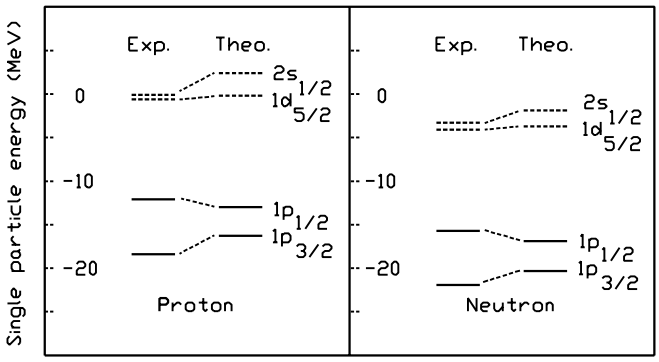

Fig. 3. Single-particle energy levels around the Fermi level for ^{16}O. The full (dotted) lines indicate filled (empty) levels.

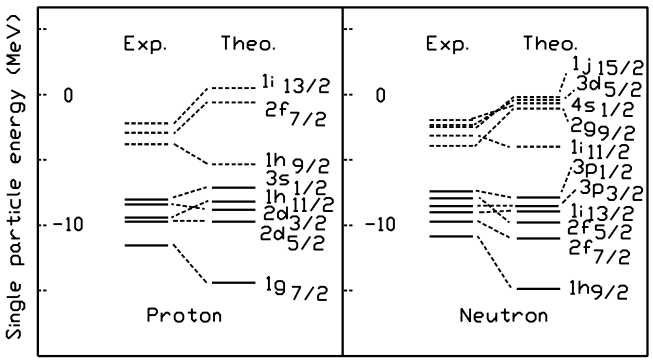

Fig. 4. Single-particle energy levels around the Fermi level for ^{208}Pb. The full (dotted) lines indicate filled (empty) levels.

tainty in the experimental charge density deep inside the nucleus. However, the description of the surface is poor compared to other conventional mean-field theories.

The spin-orbit potential, in our calculation, is stronger compared to the ZM or the ZM3 calculation as obtained in [7]. This leads to a larger spin-orbit splitting in the present model than in the conventional derivative coupling models. However, the description is still poor compared to the conventional RMF calculations and to the experiment. Figures 3 and 4 compare the theoretically predicted and the experimentally observed energies of the single-particle levels around the Fermi level of ^{16}O and ^{208}Pb, respectively.

Observing that the present approach gives a consistently good description of closed shell nuclei, we apply it to a number of singly closed shell nuclei throughout the periodic table. We have not come across any other calculation in open shell nuclei in the framework of the derivative coupling model or the hybridized derivative coupling model. A BCS calculation in the constant gap method has been applied to find out the pairing energy and the occupancies of the different levels. We confine our calculations to singly closed shell nuclei as these nuclei are expected to be very nearly spherical. The calculated binding energies are compared with the experimental values in table 3. One can see that the isotopic and isotonic trends in bind-

Table 3. Table showing binding energy and radius values calculated using the present approach as well as the experimental values for a number of singly closed shell nuclei.

Nucleus	Theoretical		Experimental	
	B.E.(MeV)	r_{ch}(fm)	B.E.(MeV)	r_{ch}(fm)
^{42}Ca	8.63	3.39	8.62	
^{44}Ca	8.61	3.40	8.66	
^{46}Ca	8.57	3.41	8.67	
^{86}Zr	8.51	4.17	8.61	
^{88}Zr	8.55	4.18	8.67	
^{92}Zr	8.57	4.21	8.69	4.30[a]
^{94}Zr	8.55	4.22	8.67	4.32[a]
^{86}Kr	8.59	4.10	8.71	
^{88}Sr	8.61	4.15	8.73	4.21[a]
^{92}Mo	8.50	4.24	8.66	4.31[a]
^{94}Ru	8.40	4.29	8.58	
^{116}Sn	8.42	4.53	8.52	4.63[b]
^{118}Sn	8.42	4.54	8.52	4.64[b]
^{120}Sn	8.40	4.56	8.50	4.65[b]
^{122}Sn	8.39	4.57	8.49	4.66[b]
^{124}Sn	8.36	4.58	8.47	4.67[b]
^{126}Sn	8.33	4.60	8.44	
^{128}Sn	8.30	4.62	8.42	
^{130}Sn	8.27	4.63	8.39	
^{204}Pb	7.77	5.40	7.88	
^{206}Pb	7.77	5.41	7.88	5.49[a]
^{210}Pb	7.75	5.43	7.84	
^{212}Pb	7.74	5.45	7.80	
^{214}Pb	7.72	5.47	7.77	

[a] Taken from the compilation [13].
[b] Data from muonic atom measurement [14].

ing energy values are reproduced in most cases although the average deviation is nearly one percent. For example, in the Sn isotopes, the difference between the calculated and the experimental binding energy per nucleon varies smoothly from 0.10 MeV to 0.12 MeV. The calculated charge radii are also compared with the experimentally observed values wherever available.

A very important quantity that changes with neutron number and has been measured very accurately is the isotopic shift $\delta\langle r^2\rangle$, *i.e.* the change in the mean-square radius with mass number. In table 4, we compare the calculated isotopic shift in the Pb isotopes with respect to ^{208}Pb with experimentally measured values. In very light nuclei, one of the main reasons for the deviation may be that these nuclei are deformed and our calculation does not take this factor into account. Isotopic shifts near the closed shell are nicely reproduced.

A better description of the different ground state properties may be obtained by changing the parameters, *viz.* the coupling constants and the meson masses. However

Table 4. Table showing isotopic shifts in the Pb isotopes with respect to ^{208}Pb.

Mass Number	Isotopic shift (fm^2)	
	Theo.	Exp.
192	−0.9031	−0.757[a]
194	−0.7870	−0.682[a]
196	−0.6696	−0.605[a]
202	−0.3183	−0.3280[b]
204	−0.2063	−0.2231[b]
206	−0.0898	−0.1179[b]
210	0.2027	0.2107[b]
212	0.3750	0.4144[b]
214	0.5520	0.6099[b]

[a] Reference [15].
[b] Reference [16].

our motivation for this paper is to check the validity of the present approach as well as the applicability of the parameters obtained in fitting the saturated nuclear matter quantities. To this extent, we have refrained from fixing the parameters by fitting the ground state properties of closed shell nuclei as is the usually followed procedure.

4 Summary and conclusions

The generalized hybrid derivative coupling model characterized by the hybridization parameter $\alpha = 1/4$ has been applied successfully to study various ground state properties of different nuclei. This model calculation gives better results, when compared with the experimental values, than the other standard model calculations, which use the same number of adjustable parameters for infinite nuclear matter as well as for finite nucleus. This model is successful in describing the ground state properties of not only the doubly closed magic nuclei (like ^{16}O, ^{40}Ca, ^{48}Ca, ^{90}Zr, ^{132}Sn, ^{208}Pb) but also those of the singly closed nuclei which are expected to be nearly spherical. A more accurate quantitative description of the ground state properties of finite nuclei may be obtained by further accurate tuning of coupling constants and meson masses which we have not done here, as we have mentioned earlier that the principal motivation of this paper is to check the applicability of the generalized hybrid derivative coupling model in the case of finite nucleus.

A part of the work has been carried out using the computer facilities provided by the DSA Programme, Department of Physics, University of Calcutta.

References

1. S. Sarkar, B. Malakar, Phys. Rev. C **50**, 757 (1994).
2. S. Sarkar, B. Malakar, Mod. Phys. Lett. A **11**, 2977 (1996).
3. B. Malakar, S. Sarkar, Prog. Theor. Phys. **98**, 600 (1997).
4. N.K. Glendenning, F. Weber, S.A. Moszkowski, Phys. Rev. C **45**, 844 (1992).
5. J. Zimanyi, S.A. Moszkowski, Phys. Rev. C **42**, 1456 (1990).
6. J.D. Walecka, Ann. Phys. (N.Y) **83**, 491 (1974); B.D. Serot, J.D. Walecka, *Advances in Nuclear Physics*, edited by J.W. Negeleo, E. Vogt, Vol. **16** (Plenum, New York, 1986).
7. M. Chiapparini, A. Delfino, M. Malheiro, A. Gattone, Z. Phys. A **357**, 47 (1997).
8. G. Hua, T.V. Chossy, W. Stocker, Phys. Rev. C **61**, 014307 (2000).
9. J. Boguta, A.R. Bodmer, Nucl. Phys. A **292**, 413 (1977) .
10. M. Rufa, P.-G. Reinhard, J.A. Maruhn, W. Greiner, M.R. Strayer, Phys. Rev. C **38**, 390 (1988).
11. P.-G. Reinhard, M. Rufa, J.A. Maruhn, W. Greiner, J. Friedrich, Z. Phys. A **323**, 13 (1986).
12. G.A. Lalazissis, M.M. Sharma, P. Ring, Nucl. Phys. A **597**, 35 (1996).
13. H. de Vries, C.W. De Jaeger, C. de Vries, At. Data Nucl. Data Tables **36**, 495 (1987).
14. C. Piller et al., Phys. Rev. C **42**, 182 (1990).
15. U. Dinger et al., Z. Phys. A **328**, 253 (1987).
16. M. Anselment, W. Faubel, S. Goring, A. Hanser, G. Meisel, H. Rebel, G. Schatz, Nucl. Phys. A **451**, 471 (1986).